Model-free Control of an Artificial Tide Generation Experimental Apparatus

Davide Tognin *, **Mirco Rampazzo** **, **Martina Pagan** ***, **Luca Carniello** *, **Alessandro Beghi** **

* *Department of Civil, Environmental and Architectural Engineering, University of Padova, Italy*
e-mail: davide.tognin@studenti.unipd.it, luca.carniello@dicea.unipd.it
** *Department of Information Engineering, University of Padova, Italy*
e-mail: {rampazzom, beghi}@dei.unipd.it
*** *I.R.S. S.r.l., Padova, Italy, e-mail: pagan@irsweb.it*

Abstract: Small-scale experiments allow to reproduce and understand phenomena and to draw inferences about large-scale processes. In this paper, we consider a peculiar experimental apparatus which is aimed at reproducing a typical lagoonal environment subject to tidal forcings. This apparatus is useful for performing morphometric analyses of synthetic tidal networks. The quality of these kind of experiments strongly depends on the behaviour of the artificial tide that has to exhibit predefined characteristics. To this aim, the height of the artificial water wave is controlled in real-time. Due to the intrinsic complexity of the system, the development of a control algorithm as simple as possible but able to ensure suitable control performance over a wide range of operative conditions, is a non-trivial task. In this paper, we have developed and tested a model-free control algorithm, that is the intelligent-PI (i-PI). Finally, the performance of the i-PI controller are compared with those of a standard regulator for different type of experiments.

Keywords: Artificial Tide Generation, PID Control, Model-free Control, Intelligent PID

1. INTRODUCTION

Tidal systems are fragile and interesting environments based on a delicate balance between sediment transport and hydrodynamics. Understanding the main processes that underlie the formation and development of tidal networks is necessary to address issues of conservation of these habitats, exposed to the effects of climate changes and human interference. In a tidal system the primary external forcing is represented by the tide. The greatest difference between tidal networks and their fluvial counterpart is that they are forced by a bidirectional flux. Indeed, the velocity is direct towards the land during the flood and towards the sea during the ebb. Therefore a difference between the velocity experienced during the two phases of the tide has an important influence on the morphology of a tidal environment. This difference is referred as tidal asymmetry and can be described using the ratio p_s between the flood peak and the ebb peak of the cross-sectionally averaged velocity. This parameter provides a distinction of the asymmetrical tidal flow into *flood dominated* ($p_s > 1$) and *ebb dominated* ($p_s < 1$). In particular, according to Tambroni et al. (2017), the nature of the flow field (i.e. flood or ebb dominance) is strictly correlated with the morphology of the tidal basin, e.g. the position of the point bars relative to the apex of a meander is strongly affected by the tidal asymmetry (Fig. 1).

Towards the goal of gaining further knowledge of some of the physical processes responsible for tidal network development under certain conditions, in particular tidal asymmetries, we set up an experimental apparatus, schematizing a back-barrier lagoonal environment subject to tidal forcings (Stefanon et al., 2010). It is worth highlight that, the chance to conduct meaningful in-scale experiments relies significantly on the characteristics of the water wave, that is generated inside the experimental apparatus and which forces the lagoon. The main contribute of this paper is the development of a control system that is able to track the reference wave signal (e.g. with fixed amplitude, period, and mean level of propagation), guaranteeing suitable performance (i.e. stability, robustness, and time-domain performance). In particular, the system should reproduce asymmetrical tides to study the effects on the morphological development of a lagoonal environment.

The considered artificial tide generation apparatus is a non-trivial system from a control point of view. Basically, it includes a water pump and a vertical sharp-edge weir, which oscillates vertically and is moved by a stepper motor. The system exhibits non-linear behaviours with fast dynamics (e.g. the electro-mechanical sub-system) and slow dynamics (e.g. the hydraulic sub-system), plus dead time (due to the water mass transport). Moreover, it is expected that certain system configurations and boundary conditions change during new campaigns of experiments. Traditional model-based control approach may be difficult to use since it is non-trivial to develop and calibrate an effective system dynamic model. Beside these aspects, we must mention that the control algorithm has to be designed under some technological constraints, given by the fact that it has to

© 2018 International Federation of Automatic Control

Fig. 1. Example of tidal meanders in the Venice Lagoon (Italy). The highlighted portions mark point bars, which are shifted seaward with respect to the apex of the meander.

be implemented as an upgrade of a traditional control unit with limited computational and memory resources.

For these reasons, we want to develop a control algorithm as simple as possible but able to ensure suitable performance, even when the system operating conditions change or if certain system parameters vary over time, avoiding tedious and time-consuming controller retuning. Specifically, we want to exploit the intelligent Proportional-Integral-Derivative (i-PID), that is a step towards a model-free control of plants with completely or partially unknown dynamics (Fliess and Join, 2009, 2013). The i-PID strategy combines a feed-forward control based on the identification of local models, which represent the plant dynamics over short periods of time, with conventional PID algorithms.

In particular, in this paper we present the application of i-PI control to the peculiar artificial tide generation experimental apparatus. The i-PI controller is developed and implemented on real hardware. The experimental results show the good performance of the i-PI controller which results appropriate to drive the artificial tide generation.

The paper is organized as follows. Section 2 outlines the experimental apparatus while Section 3 is dedicated to the design of the i-PI controller. Section 4 presents the experimental results obtained with the application of different controllers and Section 5 concludes the work.

2. EXPERIMENTAL APPARATUS

To reproduce a typical lagoonal environment we have used a large indoor apparatus, schematically depicted in Fig. 2, which consists of two adjoining basins representing the sea and a back-barrier lagoon (Fig. 2a, the plant view and Fig. 2b, a section).

The lagoon basin is 5.3 m long and 4.0 m wide, while the much deeper adjacent sea basin is 1.6 m long and 4.0 m wide. The sea is separated from the lagoon by a barrier of wooden panels, which can be moved to create inlet with different shape and position and a shelf enable us to represent the gentle slope of the sea bed in front of the lagoon. During the experiments, the lagoon is covered with a layer of sediments made of cohesionless plastic grains.

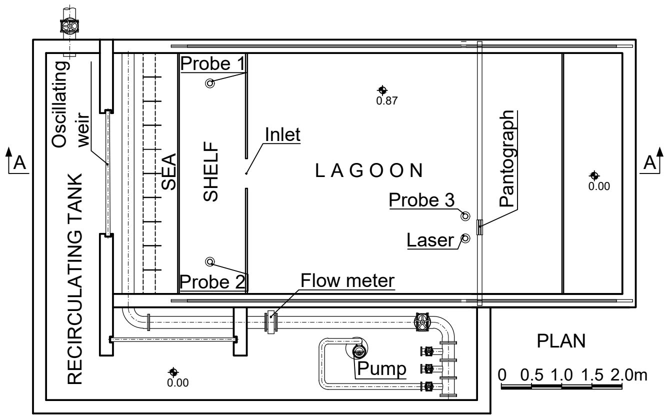

(a) Plan view: the rectangular tank, which is divided into the sea and the lagoon basin, and the recirculating tank, in which the pump is located.

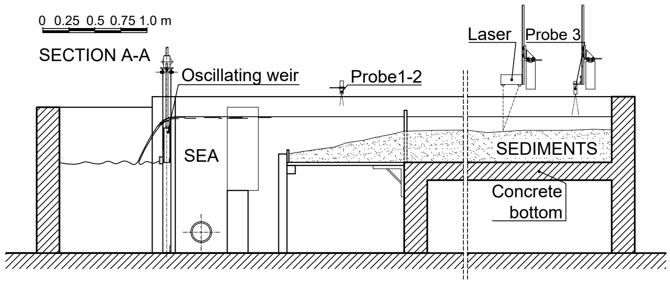

(b) Section A-A: the mechanism of water level variation and the oscillating weir.

Fig. 2. Experimental set-up.

The tide is generated at the sea by the combined action of a pump and a vertical sharp-edge weir, which is moved by a stepper motor and oscillates vertically. The water continuously flowing over the weir is collected in a separate tank, where the pump recirculates the flow.

The apparatus is equipped with two ultrasonic probes that provide a measurement of the water level in the sea, a potentiometer to measure the position of the weir and a computer driven pantograph to survey the bed elevation within the lagoon.

The wave generated at the weir does not maintain its form during the propagation to the lagoonal inlet, because of the inertia. This is the reason why the tidal wave cannot be imposed in the section of the weir but should be reproduced in front of the lagoon to be sure of the characteristic of the wave.

A block diagram of the system is depicted in Fig. 3. In broad terms, the system can be outlined as two subsystems that interact with each other in a structured manner:

- the electro-mechanical sub-system, which includes: the driver, the stepper motor, the worm gear, the lead-screw, and the sharp-edge weir;
- the water side sub-system, which includes: the water, the sea, the shelf, the lagoon, and the water pump.

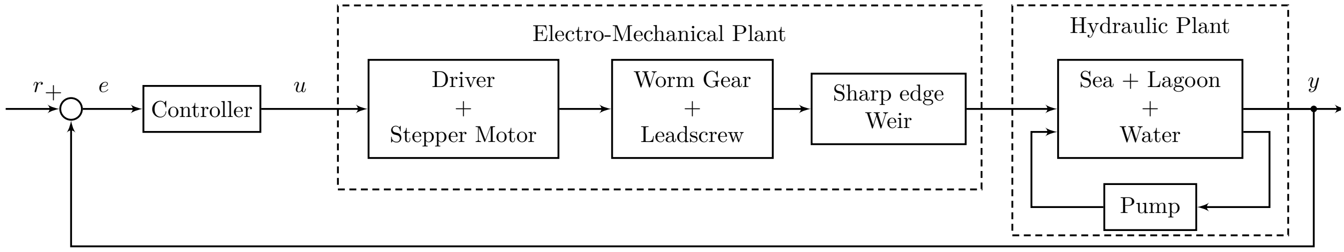

Fig. 3. The electro-mechanical sub-system main components are: the driver and the stepper motor, the worm gear with the lead-screw, and the sharp-edge weir. The hydraulic sub-system includes mainly: the sea, the lagoon, the water, and the water pump. The water level in the sea y is controlled by manipulating the stepper motor position u.

In order to conduct meaningful in-scale experiments, which rely significantly on the characteristics of tide, the water level at the sea is controlled by manipulating the stepper motor position, which in turn, determines the sharp-edge weir height position, while the water pump is set to a fixed flow rate.

3. MODEL-FREE CONTROL

The artificial tide generation system exhibits non-linear behaviours with both fast dynamics (e.g. the electro-mechanical sub-system) and slow dynamics (e.g. the hydraulic sub-system), plus dead time (due to the water mass transport). It is also expected that certain system configurations, boundary conditions, and some system parameters may change during campaigns of experiments. Moreover, the control algorithm for the artificial tide generation apparatus has to be designed under some technological constraints, given by the fact that it has to be implemented as an upgrade of a traditional control unit, with limited computational and memory resources. From a practical point of view, the use of a standard regulator sounds good. On the other hand, due to the difficulty in adopting a model-based control approach and/or in setting-up trial-and-error experiments for tuning PID parameters by inspecting the dynamic behaviour of the process output, we here adopt a model-free control approach, that is the intelligent PI (Fliess and Join, 2009; Join et al., 2010; D'Andréa-Novel et al., 2010; Fliess and Join, 2013; Rampazzo et al., 2017).

This type of control technique is based on an elementary continuously update local modelling via the unique knowledge of the system input-output behaviour. By way of example, we consider a SISO system approximately governed by an unknown finite-dimensional ordinary differential equation:

$$E\left(t, y, \frac{dy}{dt}, ..., \frac{d^n y}{dt^n}, u, \frac{du}{dt}, ..., \frac{d^m u}{dt^m}\right) = 0, \qquad (1)$$

where u and y are the input and output variables respectively, whereas E is assumed to be a sufficiently smooth function such as:

$$\frac{\partial E}{\partial \dot{y}} \neq 0. \qquad (2)$$

According to the Dini's implicit function theorem the system (1) can locally be rewritten as follows:

$$\dot{y} = \mathcal{E}\left(t, \frac{d^2 y}{dt^2}, ..., \frac{d^n y}{dt^n}, u, \frac{du}{dt}, ..., \frac{d^m u}{dt^m}\right), \qquad (3)$$

that leads to the following phenomenological ultra-local model:

$$\dot{y} = F + \alpha u. \qquad (4)$$

In (4), F contains all structural information of the process while $\alpha \in \mathbb{R}$ is a non-physical parameter, which is typically chosen iteratively, such that F and αu are of the same magnitude.

We choose the closed-loop controller such as:

$$u = -\frac{\hat{F} - \dot{r} - \mathcal{C}(e)}{\alpha}, \qquad (5)$$

in which, the estimation of the structural information of the process is computed, by means of (4), as follows:

$$\hat{F} = \dot{y} - \alpha u. \qquad (6)$$

Furthermore, in (5), r is the output reference trajectory, and $e = r - y$ is the tracking error, Fig. 4. The controller $\mathcal{C}$ should be selected such that a perfect tracking is asymptotically ensured, i.e.:

$$\lim_{t \to +\infty} e(t) = 0. \qquad (7)$$

By combining (4) and (5), we obtain:

$$\dot{e} + \mathcal{C}(e) = 0. \qquad (8)$$

It is worth pointing out that F does not appear anymore in (8), i.e. the unknown parts and disturbances of the plant vanish. The tracking condition expressed by (7) is easily fulfilled by choosing, for example, a standard PI (Proportional-Integral) regulator as $\mathcal{C}$:

$$\mathcal{C}(e(t)) = K_{ip}\left(e(t) + \frac{1}{T_{ii}} \int_0^t e(\tau) d\tau\right). \qquad (9)$$

The tuning of PI parameters becomes therefore straightforward for obtaining a good tracking of the reference. This is a major benefit when compared to the tuning of classic standard regulator. Roughly speaking, the intelligent PI can be regarded as a feed-forward control based on the local plant models in combination with a conventional PI algorithm.

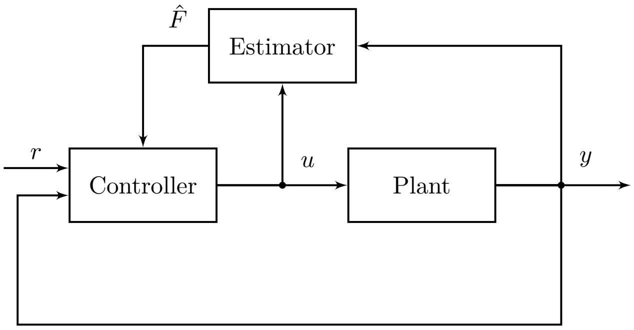

Fig. 4. Model-free control architecture; r is the reference signal, y is the process output, $\hat{F}$ is an estimation of the structural information of the process, and u is the actuating signal generated by the controller.

3.1 Estimation of the Process Structural Information

In order to estimate the structural information of the process $\hat{F}$ from (6), it is crucial to have available a good estimate of the differentiation of the output y with respect to time. In particular, the $\dot{y}$ can be inferred by using a peculiar feedback loop where the output of an integrator (i.e. 'the plant') has to track the reference y, Fig. 5. As a consequence, the integrator input can be regarded as an estimate for $\dot{y}$ (Horn and Reichhartinger, 2009). In particular, a robust exact differentiator scheme is used (Levant, 1998), where the controller C implements the so-called super-twisting algorithm (Levant, 2007):

$$\hat{\dot{y}} = z - \varphi\sqrt{|\xi|}\ \mathrm{sign}(\xi), \tag{10a}$$
$$\dot{z} = -k\ \mathrm{sign}(\xi), \tag{10b}$$

where z is an auxiliary variable, whereas φ and k are positive constants. It is worth highlighting that, thanks to this approach, the error ξ as well as its first time-derivative are forced to zero in finite time (Levant, 2003).

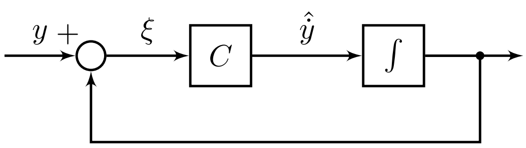

Fig. 5. Robust exact differentiator scheme.

4. EXPERIMENTAL RESULTS

4.1 Sinusoidal Tide Reference

By way of an example, we consider as tide reference a sinusoidal signal with amplitude equal to 0.75 [cm] and period equals 8 [min]. In particular, we compare the performance of a standard PID regulator (Aström and Hägglund, 2006; Visioli, 2006) and that of an intelligent-PI controller, which have been tuned via trial-and-error procedures. The parameters of the controllers are shown in Table 1. In Fig. 6a we can see the reference signal (the dashed black line), the output provided by the standard regulator (the red line), and the output provided by the i-PI controller (the blue line). The intelligent PI is able to satisfactory tracks the reference, on the contrary by using the standard regulator the output is lagging behind the reference. The tracking error e and the controller output u, for both controllers, are depicted in Fig. 6b and Fig. 6c, respectively. The PID controller exhibits an ITSE (Integral Time Squared Error) equal to 55060 [cm^{2}s] while the i-PI controller entails an ITSE equals 9980 [cm^{2}s], that is about 5 times smaller.

Table 1. Controllers parameters.

PI	i-PI
$K_p = 150 \cdot 10^3$ [step · cm ^{1}]	$K_{pi} = 175$ [step · cm ^{1}]
$T_i = 7$ [s]	$T_{ii} = 1$ [s]
	$\alpha = 5 \cdot 10$ ^{3} [cm s ^{1} step ^{1}]

4.2 Ebb-dominated and Flood-dominated Tide References

In these experimental examples we consider more realistic references for the tide and the considered on-board controller is the i-PI one. Fig. 7 depicts some results concerning the ebb-dominated reference, while Fig. 8 refers to the flood-dominated case. In particular, Fig. 7a and Fig. 8a show the height of the tide provided by the ultrasonic probe (the blue line) and the sharp-edge weir vertical position provided by the potentiometer (the cyan line). For the the ebb-dominated tide, the output, which follows the reference with a small error (less or equal then about 0.1 [cm], Fig. 7b) and the ITSE, that is equal to 10874 [cm^{2}s], confirm the satisfactory performance of the i-PI controller. The same can be said for the flood-dominated wave, which presents an ITSE equal to 10867 [cm^{2}s] and an error again less the about 0.1 [cm] (Fig. 8b). Furthermore, the sharp-edge weir vertical position signal (the cyan line) presents an anticipation and an higher value of amplitude with respect to the tidal wave effectively generated (the blue line), due to the fact that the wave changes its form during the propagation from the weir to the lagoonal inlet. This observation restates the necessity of generate the desired wave directly in front of the lagoon in order to avoid unwanted transformation, that results in the impossibility of ensuring certain tidal forcing characteristics at the lagoonal inlet. Fig. 7c and Fig. 8c show the value of the manipulated variable u, calculated by the i-PI as input for the stepper-motor driver, for the ebb-dominated and the flood-dominated tide, respectively. It is perhaps worth stressing that smooth profiles of u avoid unwanted additional stresses on the stepper-motor and contribute to a longer life of the mechanical components.

5. CONCLUSION

In this paper, we have compared the performance of a standard regulator with those of an i-PI for controlling the shape of an artificial tidal wave generation system, that is one of the main component in an experimental apparatus which is devoted to the study of the morphodynamic development of lagoonal environments. The intelligent PI can be regarded as a feed-forward control based on the local plant models in combination with a conventional PI algorithm. For these reasons the i-PI reaches a satisfactory balance between performance and architectural complexity. We have conducted various tests on the experimental apparatus by reproducing flood dominated and ebb dominated tidal flows. From the experimental tests, we can conclude that the performance of the i-PI model-free controller is ever better than that of the standard regulator. In particular, the use of this model-free approach allows to adequately control the system without resorting to tedious and time-consuming controller retuning when changes of the system operating conditions or time-varying parameters arise.

REFERENCES

Aström, K.J. and Hägglund, T. (2006). *Advanced PID control*. ISA, Advanced PID control.

D'Andréa-Novel, B., Fliess, M., Join, C., Mounier, H., and Steux, B. (2010). A mathematical explanation via "intelligent" PID controllers of the strange ubiquity of PIDs. In *Control Automation (MED), 2010 18th Mediterranean Conference on*, 395–400.

Fliess, M. and Join, C. (2009). Model-free control and intelligent pid controllers: Towards a possible trivialization of nonlinear control? *IFAC Proceedings Volumes*, 42(10), 1531–1550.

Fliess, M. and Join, C. (2013). Model-free control. *International Journal of Control*, 86(12), 2228–2252.

Horn, M. and Reichhartinger, M. (2009). Model-free control of a thermal plant. In *Control and Automation, 2009. ICCA 2009. IEEE International Conference on*, 1839–1843. IEEE.

Join, C., Robert, G., and Fliess, M. (2010). Model-free based water level control for hydroelectric power plants. In *IFAC Conference on Control Methodologies and Tecnologies for Energy Efficiency, CMTEE*. IFAC, Vilamoura, Portugal.

Levant, A. (1998). Robust exact differentiation via sliding mode technique. *Automatica*, 34(3), 379–384.

Levant, A. (2003). Higher-order sliding modes, differentiation and output-feedback control. *International Journal of Control*, 76(9-10), 924–941.

Levant, A. (2007). Principles of 2-sliding mode design. *Automatica*, 43(4), 576–586.

Rampazzo, M., Cervato, A., and Beghi, A. (2017). Remote refrigeration system experiments for control engineering education. *Computer Applications in Engineering Education*, 25(3), 430–440.

Stefanon, L., Carniello, L., D'Alpaos, A., and Lanzoni, S. (2010). Experimental analysis of tidal network growth and development. *Continental Shelf Research*, 30(8), 950–962.

Tambroni, N., Luchi, R., and Seminara, G. (2017). Can tide dominance be inferred from the point bar pattern of tidal meandering channels? *Journal of Geophysical Research: Earth Surface*, 122(2), 492–512.

Visioli, A. (2006). *Practical PID Control*. Springer-Verlag.

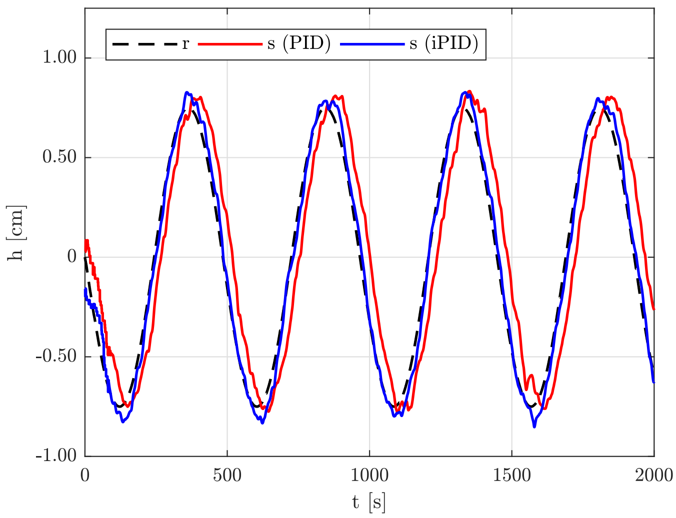

(a) The reference r and the output y. PID vs. i-PI.

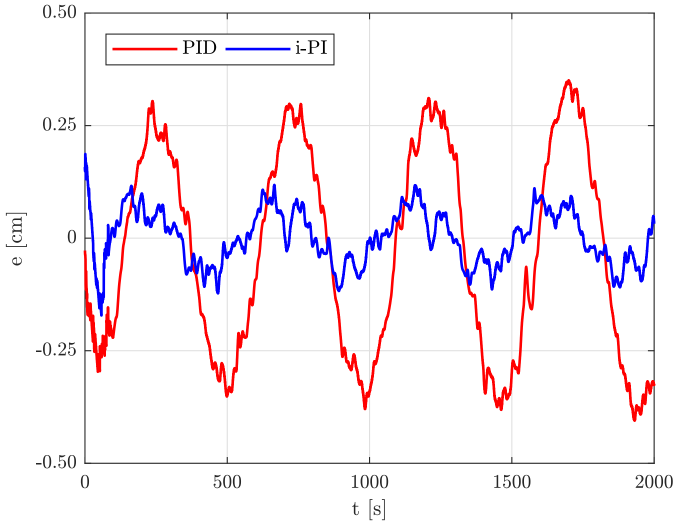

(b) The error between the reference and the output. PID vs. i-PI.

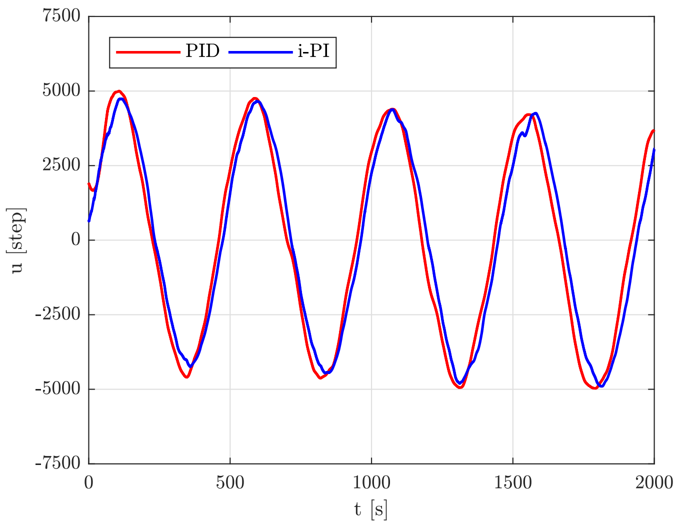

(c) Manipulated variable u, i.e. the input stepper-motor driver. PID vs i-PI.

Fig. 6. Comparison between the results obtained with a standard PID and an i-PI controller, tested on a sinusoidal wave.

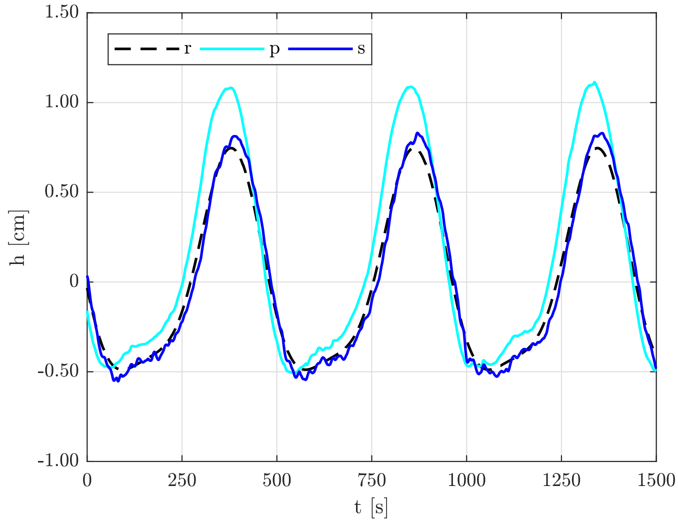

(a) Comparison between the reference signal r, the water level measured by the ultrasonic probe s and the weir position measured by the potentiometer p.

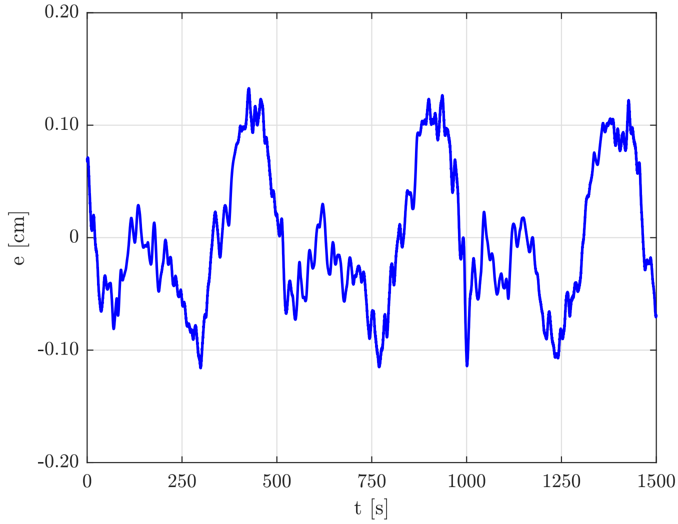

(b) The error between the reference and the output.

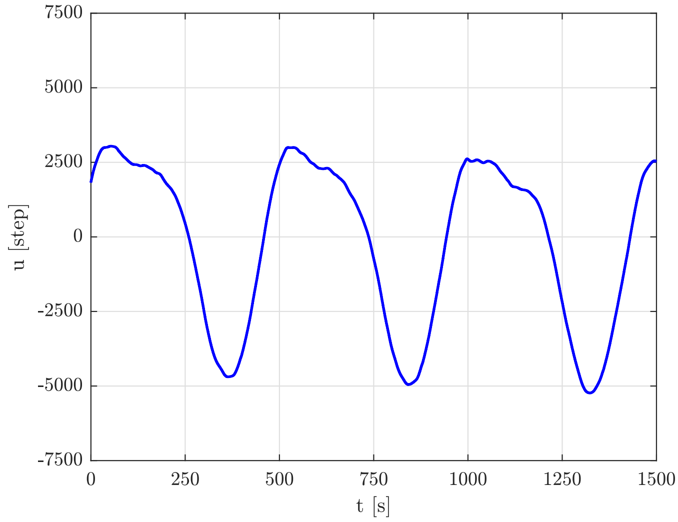

(c) Manipulated variable u, i.e. the input stepper-motor driver.

Fig. 7. Results obtained with the generation of an ebb-dominated tidal wave.

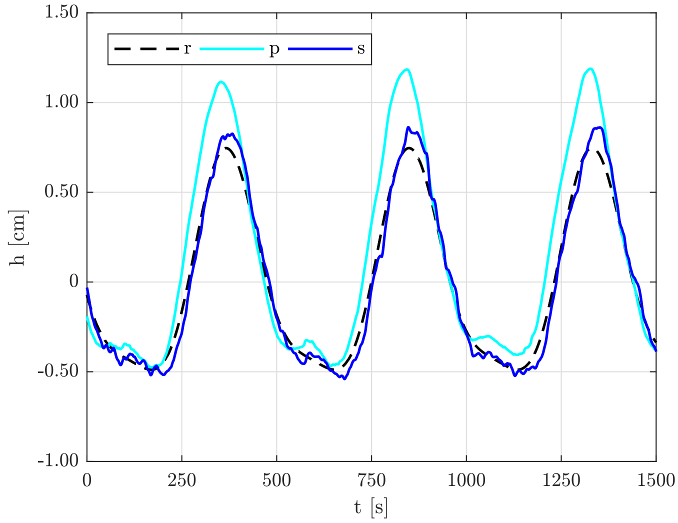

(a) Comparison between the reference signal r, the water level measured by the ultrasonic probe s and the weir position measured by the potentiometer p.

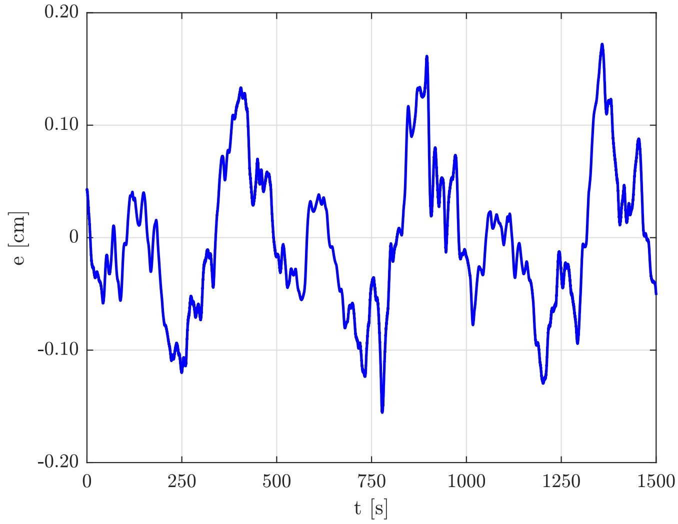

(b) The error between the reference and the output.

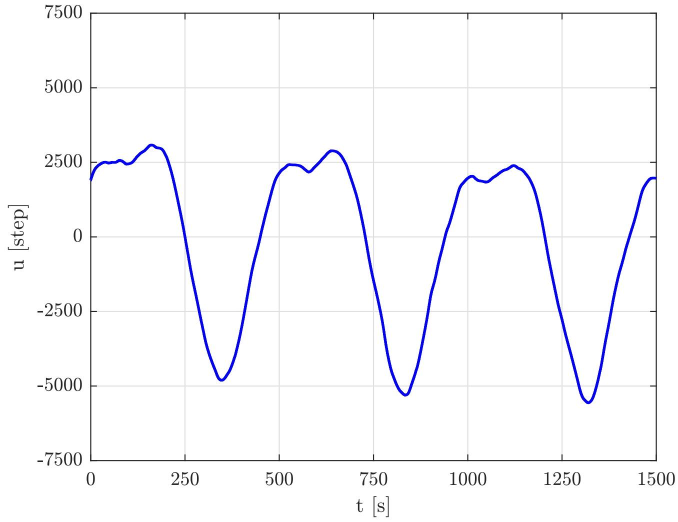

(c) Manipulated variable u, i.e. the input stepper-motor driver.

Fig. 8. Results obtained with the generation of an flood-dominated tidal wave.